A Conservative Multi-block Algorithm for Two-dimensional Numerical Model

Yaoxin Zhang, Yafei Jia, and Sam S.Y. Wang

Abstract—A multi-block algorithm and its implementation in two-dimensional finite element numerical model CCHE2D are presented. In addition to a conventional Lagrangian Interpolation Method (LIM), a novel interpolation method, called Consistent Interpolation Method (CIM), is proposed for more accurate information transfer across the interfaces. The consistent interpolation solves the governing equations over the auxiliary elements constructed around the interpolation nodes using the same numerical scheme used for the internal computational nodes. With the CIM, the momentum conservation can be maintained as well as the mass conservation. An imbalance correction scheme is used to enforce the conservation laws (mass and momentum) across the interfaces. Comparisons of the LIM and the CIM are made using several flow simulation examples. It is shown that the proposed CIM is physically more accurate and produces satisfactory results efficiently

Keywords—Multi-block Algorithm; Conservation; Interpolation; Numerical model; Flow simulation.

I. INTRODUCTION

NUMERICAL simulation of flows in complex geometries remains a challenge in the Computational Fluid Dynamics (CFD). One difficulty lies in the discretization of the physical domain with a computational mesh, while another is to conduct the simulations efficiently and accurately. The resulting mesh generated using single-block method in these cases is often highly deformed with large blanked areas. The multi-block method, an approach which divides a complicated domain into several sub-domains (blocks) with simpler shapes, can alleviate the above difficulties significantly. It has been applied widely and successfully in CFD. Benek et al. [1], Hessinius and Rai [13], Rai [23, 24] and Wang [31] applied it to the Euler equations; Gresho and Sani [10], Furukawa et al. [9], Klopfer and Molvik [18], Steger [29], Wright and Shyy [34], Henshaw [12], Sheng et al. [27], Sinha et al. [28] and Brakkee [3] succeeded in applying it to the Navier-Stokes equations; Chen and Chen [5], and Chen and Liu [6] studied the turbulent flow

Yaoxin Zhang is with the National Center for Computational Hydroscience and Engineering, MS 38677 USA (phone: 662-915-3960; fax: 662-915-7796; e-mail: yzhang@ ncche.olemiss.edu).

Yafei Jia, is with the National Center for Computational Hydroscience and Engineering, MS 38677 USA (e-mail: jia@ncche.olemiss.edu).

Sam S.Y. Wang is with the National Center for Computational Hydroscience and Engineering, MS 38677 USA (e-mail: wang@ncche.olemiss.edu).

around a ship using the multi-block algorithm; Meakin [19], and Meakin and Street [20] applied it to the simulation of the environmental flow; Sheng [27] used this method to study the turbulent flow about the appended submarine configurations; Tu and Fuchs [30] simulated the unsteady flow in an internal combustion machine; and, Francisco and Sabadell [8] developed a multi-block method to study the elastic wave propagation problems.

The use of the multi-block approach introduces new boundaries inside the solution domain: the inter-block boundaries. Accordingly, a multi-block mesh consists of two kinds of nodes: the computational nodes that discretize the governing equations, and the interpolation nodes located on the inter-block boundaries. The variables at the interpolation nodes are interpolated from the computational nodes of the neighboring blocks. A multi-block algorithm is basically composed of two main parts: (1) an interpolation method to transfer information between neighboring blocks; and (2) a conservation strategy to enforce the conservation laws across the interfaces.

Conventionally, the information transfer between the neighboring blocks is fulfilled by the Lagrangian Interpolation Method (LIM), in which an interpolation stencil is constructed. For examples, Meakin [19] used a tri-quadratic LIM, Perng and Street [22] used a bilinear LIM, Tu and Fuchs [30] constructed a $4 \times 4 \times 4$ interpolation stencil, and Zang and Street [36] used a bi-quadratic LIM, etc. Unless the conservation constraints are involved in the derivation, the LIM is non-conservative.

It has been generally accepted that the global mass conservation is critical for the convergence as well as the accuracy of the incompressible flow. In order to reduce the error introduced by the non-conservative interpolations, a conservation strategy must be applied. Meakin [19] proposed an imbalance correction scheme (IC) to enforce the mass conservation. That is, the amount of the mass residual in a given block is subtracted and redistributed along the inter-block boundary. In addition to mass, the IC can be applied to the other conservative quantities as well. Compared to the mass conservation, the momentum conservation across the interfaces has not been considered so important that it would influence the convergence of the computation. Therefore, it is often ignored in the study of the multi-block algorithm. Caruso [4] stated that it is nearly impossible and very difficult to conserve additional quantities, such as momentum, energy, etc. One major difficulty lies in the lack of the accurate evaluation

of those quantities at the interfaces. Moon and Liou [21] used the Van Leer's [31] flux-vector splitting procedures to evaluate the numerical flux at the interfaces and then used a high order redistribution scheme with the area-weighted coefficients to enforce the conservation laws. Klopfer and Molvik [18] showed that the numerical flux must be determined by the same numerical scheme as used in the model; otherwise discrepancies or inconsistencies may occur at the interfaces.

In the present study, a conservative multi-block algorithm is proposed for a two-dimensional hydrodynamic model, the CCHE2D model. In addition to a nine-node second-order quadratic LIM, a Consistent Interpolation Method (CIM) is developed. Using the CIM, the momentum equations are solved on the velocity interpolation nodes along the block interfaces in the same way as the internal velocity computational nodes; while the continuity equation is solved on the pressure computational nodes within the overlapping zone. With the IC scheme, the CIM is capable of maintaining both the momentum conservation and the mass conservation along the interfaces. Several test examples show that the proposed multi-block algorithm can yield good results with high efficiency.

II. NUMERICAL MODEL

The present multi-block algorithm is applied to a two-dimensional hydrodynamic and sediment transport model for unsteady open channel flows over loose bed, CCHE2D model. Here a brief introduction of the CCHE2D model is presented and its details can be found in Jia and Wang [14~16].

A. Governing Equations

The depth integrated two-dimensional equations solved in CCHE2D model are as follows.

Continuity Equation:

$$\frac{\partial Z}{\partial t} + \frac{\partial(hu)}{\partial x} + \frac{\partial(hv)}{\partial y} = 0 \tag{1a}$$

or in the integral form:

$$\frac{\partial Z}{\partial t} + \frac{1}{A}\oint h\vec{U}\,d\vec{s} = 0 \tag{1b}$$

Momentum Equations:

$$\frac{\partial u}{\partial t} + u\frac{\partial u}{\partial x} + v\frac{\partial u}{\partial y} = \tag{2}$$
$$-g\frac{\partial Z}{\partial x} + \frac{1}{h}[\frac{\partial(h\tau_{xx})}{\partial x} + \frac{\partial(h\tau_{xy})}{\partial y}] - \frac{\tau_{bx}}{\rho h} + f_{Cor}v$$

$$\frac{\partial v}{\partial t} + u\frac{\partial v}{\partial x} + v\frac{\partial v}{\partial y} = \tag{3}$$
$$-g\frac{\partial Z}{\partial y} + \frac{1}{h}[\frac{\partial(h\tau_{yx})}{\partial x} + \frac{\partial(h\tau_{yy})}{\partial y}] - \frac{\tau_{by}}{\rho h} - f_{Cor}u$$

where u and v are the depth-integrated velocity components in the x and y directions respectively; g is the gravitational acceleration; Z is the water surface elevation; ρ is water density; h is the local water depth; f_{Cor} is the Coriolis parameter; τ_{bx} and τ_{by} are shear stresses on the bed surface, and $\tau_{xx}, \tau_{xy}, \tau_{yx}$ and τ_{yy} are the depth integrated Reynolds stresses, which are approximated based on Boussinesq's assumption:

$$\tau_{xx} = 2\nu_t\frac{\partial u}{\partial x} \tag{4a}$$

$$\tau_{xy} = \tau_{yx} = \nu_t(\frac{\partial u}{\partial y} + \frac{\partial v}{\partial x}) \tag{4b}$$

$$\tau_{yy} = 2\nu_t\frac{\partial v}{\partial y} \tag{4c}$$

where the eddy viscosity ν_t is calculated by two eddy viscosity models, the depth-integrated parabolic model and the depth-integrated mixing-length model, in this version of CCHE2D model.

B. Discretized Equations

The numerical method used in CCHE2D model is called the Efficient Element Method (EEM). A partially staggered structured mesh system is used to solve the governing equations (Jia et al. [17]). The velocity components are solved at the collocation nodes, while the pressure (water-surface-correction) is solved at the centers of the cells. A quadratic interpolation function for nine-node element is constructed to discretize the momentum equations, while the continuity equation solved at the staggered nodes requires a bilinear interpolation function and a quadratic interpolation function (see Figure 1).
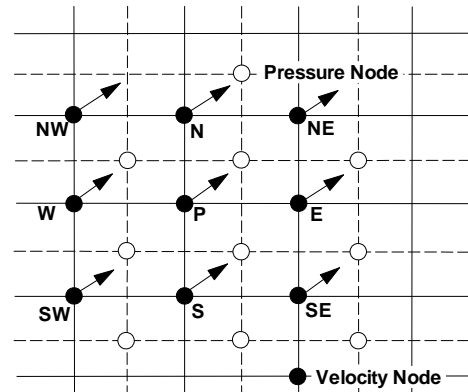

Fig.1 The nine-node element and the four-node element in a partially staggered mesh

The compact forms of the explicit discretization of the continuity equation and the momentum equations are simply listed as follows,

$$Z'^{n+1} = \Delta t \cdot Q^n + \Delta t \cdot FS^n \qquad (5)$$

$$u^{n+1} = u^n + \Delta t \cdot C_u^n + \Delta t \cdot FM_u^n \qquad (6a)$$

$$v^{n+1} = v^n + \Delta t \cdot C_v^n + \Delta t \cdot FM_v^n \qquad (6b)$$

where Z' is the correction of water surface elevation, Δt is the time step, n is the time level, Q is the divergence term and FS is the source term, the convective terms C_u and C_v are the discretized advection terms on the left side of Equations (2) and (3); FM_u and FM_v are the discretized momentum forcing terms (the pressure gradient, the Reynolds stresses, the shear stresses and the Coriolis force term) on the right side of Equations (2) and (3).

A pressure correction method is used to couple the velocity and the pressure field. The velocity is corrected by the pressure (water surface) correction term to enforce mass conservation as follows:

$$\vec{u}^{n+1} = \vec{u}^* - \Delta t \cdot g \cdot \nabla Z' \qquad (7a)$$

$$Z' = Z^{n+1} - Z^n \qquad (7b)$$

where $\vec{u}^*$ is provisional velocity and Z is water surface elevation.

III. MULTI-BLOCK ALGORITHM

The treatment of the inter-block boundaries is the key to the success of a multi-block algorithm. It has to address two important issues: the information transfer and the conservation strategy.

A. Multi-block Mesh System

As shown in Figure 2, the present multi-block algorithm is based on a simple overlapping mesh system, in which an overlapping zone and two interfaces lay between two neighboring blocks. In this system the mesh lines can be discontinuous across the interfaces, the distributions of the mesh lines of the two neighboring blocks are independent of each other.
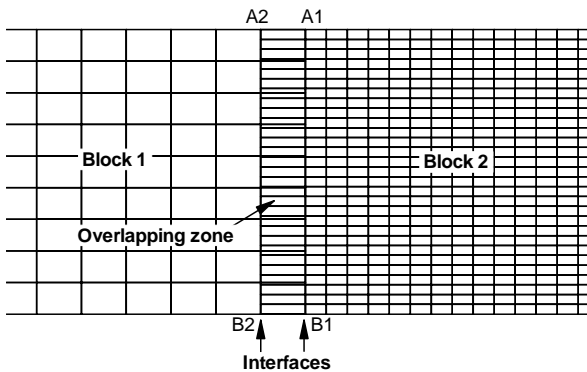

Fig. 2 A Two-block Mesh

B. Information Transfer

The LIM is often used to transfer information across the interfaces. It is based on the assumed distributions for the variables to be interpolated and the interpolated results vary with the spatial distribution of the interface and mesh. It is therefore not necessarily consistent to the numerical solutions. As a result, the LIM is non-conservative, if no additional conservation condition or constraint is enforced in the derivation of the scheme. To remedy this, a new interpolation method, the *Consistent* Interpolation Method (CIM), is proposed in this study. To make them consistent with the internal computational nodes, the interpolation nodes should be treated in the same way as those computational nodes. That is, the governing equation should also be solved at the interpolation nodes using the same numerical method as that for computational nodes. To achieve this, auxiliary elements are constructed around the interpolation nodes.

In the present study, the CIM is used for the momentum equations. As can be seen (Figures 3 and 4), the auxiliary elements (A and B) are composed of velocity interpolation nodes, velocity computational nodes, pressure computational nodes, velocity auxiliary nodes, and pressure auxiliary nodes. For example, in element A, nodes NW, N, and NE are velocity computational nodes; W, P, E are velocity interpolation nodes; and SW, S, and SE are velocity auxiliary nodes. The auxiliary elements are beyond the blocked mesh system and constructed by extending the mesh lines at the interfaces into the neighboring block.

Applying the momentum equations to the constructed element, one can obtain the *consistent* interpolation for the velocity on the interpolation node P' as follows:

$$u_{P'}^{n+1} = u_{P'}^n + \Delta t \cdot (C_u)_{P'} + \Delta t \cdot (FM_u)_{P'} \qquad (8a)$$

$$v_{P'}^{n+1} = v_{P'}^n + \Delta t \cdot (C_v)_{P'} + \Delta t \cdot (FM_v)_{P'} \qquad (8b)$$

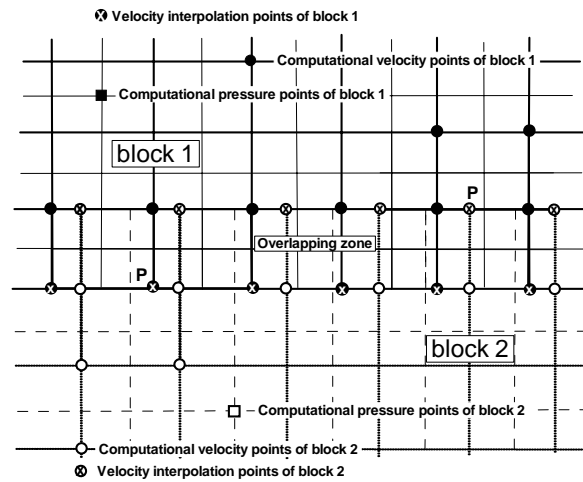which has the same form as Equation (6).
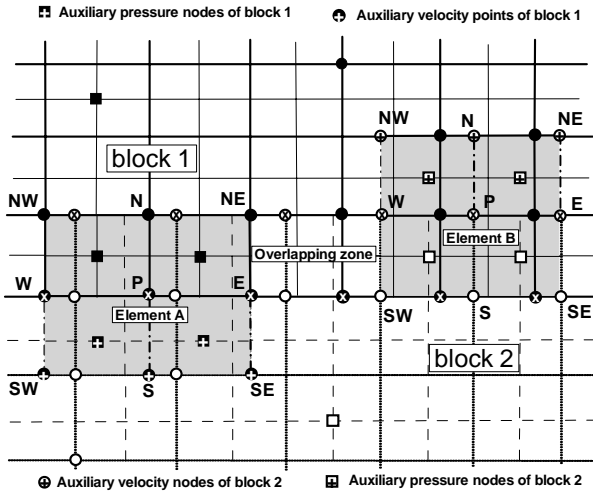

Fig. 3 Consistent interpolation: a two-block mesh

Fig. 4 Consistent interpolation: auxiliary elements

In Equation (8), the convective terms and the momentum forcing terms contain the information from the auxiliary velocity nodes and the auxiliary pressure nodes, which are obtained by the LIM.

C. Conservation Strategy

The LIM is in general non-conservative. As for the CIM, governing equations are discretized and solved at the interpolation nodes. It inherits the physical characteristics of the governing equations. However, it is non-conservative either due to the fact that the solutions on the auxiliary nodes are interpolated with the LIM. In order to reduce the error of the non-conservative interpolation, a conservation strategy must be applied. Meakin [19] proposed an imbalance correction scheme (IC) to redistribute the mass residual along the inter-block boundary to enforce the mass conservation, while Moon and Liou [21] redistributed the total amount instead of the residual (or discrepancy) using an area-weighted scheme. In this study, the IC scheme is adopted to maintain the conservation laws. In a two-block mesh as shown in Figure 2, for any quantity q (i.e., u, v, Z') across the interfaces, the IC scheme for block 1 can be described as follows.

$$q_{1,i}^{C} = q_{1,i}^{old} + w_j \cdot \varepsilon_q \qquad (9a)$$

$$\varepsilon_q = \int_D q_2 dD - \int_D q_1 dD \qquad (9b)$$

where the subscript "$1, j$" denotes the local value of q at node j of block 1; the superscript "C" denotes the corrected value; D denotes the interface or the overlapping zone; and w_j is the local distribution weight.

To evaluate the distribution weight, it is assumed that the introduced local error is proportional to the local value, so is the correction. With this assumption, Zang and Street [36] used the following formula to distribute the residual.

$$w_j = \frac{|q_j|}{\sum |q_j|} \qquad (9c)$$

D. Mass Conservation

In Figure 2, along the interface A1-B1, the local flux of block 1 can be corrected using the IC scheme.

$$f_{1,i}^{C} = f_{1,i}^{old} + \frac{|f_{1,i}^{old}|}{\sum |f_{1,i}^{old}|} \cdot \varepsilon_f \qquad (10a)$$

$$\varepsilon_f = \int f_2 dl - \int f_1 dl \qquad (10b)$$

where l denotes the interface A1-B1 of block 1 and block2.

Similarly, according to IC scheme and Equation (5), the local water-surface-correction Z' of block 1 within the overlapping zone can be corrected by the following equation.

$$Z_{1,i}^{'C} = Z_{1,i}^{'old} + \Delta t \cdot \frac{|Q_{1,i}^{old} \cdot A_j|}{\sum |Q_{1,i}^{old} \cdot A_j|} \cdot \varepsilon_D \qquad (11a)$$

$$\varepsilon_D = \int_D Q_2 dD - \int_D Q_1 dD \qquad (11b)$$

where A_j is the local cell area.

For the LIM, Equations (10) and (11) are essential to maintain the mass conservation across the interfaces.

E. Momentum Conservation

Compared to the mass conservation, the momentum conservation across interfaces is more difficult to preserve. To maintain the momentum conservation, first of all, an accurate estimation method of the momentum flux at the interface is needed. According to the studies of Klopfer and Molvik [18], in order to avoid the discrepancies or inconsistencies at the interfaces, the numerical flux should be determined by the same numerical scheme as used in the model. Moon and Liou [21] used the Van Leer's [31] flux-vector splitting procedures to evaluate the numerical flux at the interfaces. In the current study, with the CIM, preserving the momentum conservation can be enforced easily.

The discretization of the momentum equation (6) can be rewritten as follows:

$$\rho V \cdot a_u = \rho V \cdot [\frac{u^{n+1} - u^n}{\Delta t} - (C_u)^n] = \qquad (12a)$$

$$\rho V \cdot (FM_u)^n$$

$$\rho V \cdot a_v = \rho V \cdot [\frac{v^{n+1} - v^n}{\Delta t} - (C_v)^n] = \qquad (12b)$$

$$\rho V \cdot (FM_v)^n$$

where $V (= Ah)$ is cell volume, ρV is the mass of the cell; a_u and a_v are the total accelerations in the x and y direction, respectively.

According to Equations (9) and (12), the momentum discrepancies in the *x* and *y* direction along the interface A1-B1 can be distributed as follows.

$$u_{1,i}^C = u_{1,i}^{old} + \Delta t \cdot \frac{|(FM_u)_{1,i}^{old}|}{\sum |(FM_u)_{1,i}^{old} \cdot V_i|} \cdot \varepsilon_u \qquad (13a)$$

$$v_{1,i}^C = v_{1,i}^{old} + \Delta t \cdot \frac{|(FM_v)_{1,i}^{old}|}{\sum |(FM_v)_{1,i}^{old} \cdot V_i|} \cdot \varepsilon_v \qquad (13b)$$

$$\varepsilon_u = \int (FM_u)_2 \, dV - \int (FM_u)_1 \, dV \qquad (13c)$$

$$\varepsilon_v = \int (FM_v)_2 \, dV - \int (FM_v)_1 \, dV \qquad (13d)$$

Equation (13) is used to correct local velocity to enforce momentum conservation along the interfaces. Since the discrepancies or residuals in Equations (11) and (13) are caused by the auxiliary nodes whose solutions are obtained by the LIM, these two equations are capable of removing the errors from the auxiliary nodes. For the pressure nodes within the overlapping zone, Equation (5) (discretized continuity equation for the computational pressure nodes) and Equation (11) (IC for mass conservation) are solved; while for the velocity interpolation nodes along the interfaces, Equations (8) and (13) are solved, which are comparable to Equation (6) (discretized momentum equations for the computational velocity nodes). Equation (7) is also applied to the velocity interpolation nodes along the interfaces. The above solution procedure for the interpolation nodes along the interfaces is therefore consistent with that of other computational nodes. It is conservative both in mass and momentum.

F. Comparisons of LIM and CIM

The LIM has been widely and successfully applied in the study of the multi-block algorithm [1-13, 18-24, 27-34 and 36]. It is simple and easy to implement, but it is only based on the assumed spatial distribution without considering the flow physics.

As for the CIM, since it solves the governing equations over the auxiliary elements, it is more complicated and needs more computational efforts. However, the CIM is based on the governing equations which are derived according to the conservation laws. With the help of the IC method (Equations (11) and (13)), the CIM can inherit the physical characteristic (i.e., conservation) of the numerical method used for the computational nodes.

IV. EXAMPLES AND DISCUSSIONS

This section presents the validation of the present multi-block algorithm and its implementation to the explicit version of CCHE2D model, in which two zero-equation eddy viscosity models are available. For illustration purposes, the following domains are considered as "geometrically complex": a straight channel, a straight channel with a spur dike, a bifurcation channel, and a sudden-expansion channel. The mixing length turbulence closure model is used for all examples.

Note that turbulent flows are complicated, and many factors play important roles in the accuracy of numerical simulations, such as the numerical scheme, mesh resolution, turbulence closure schemes etc. The multi-block algorithm is only a special technique to enhance the capability and efficiency of the numerical models to handle the geometrically complex domains. It cannot replace or compensate for the other important factors, especially the turbulence closure schemes.

A. Straight Channel

A simulation of a steady subcritical flow in a straight channel is used to validate the correctness of the connectivity at the interfaces. This straight channel is 3.3m long and 0.5m wide with a flat bed. The Manning resistant coefficient is 0.011. The water surface elevation of 0.055m is imposed at the downstream end, while a discharge of 0.01m³/s is imposed on the upstream end of the channel. As shown in Figure 5, the whole channel is decomposed into three blocks with mesh sizes are 20×10, 29×30, and 20×20.

The flow structure in this channel is quite simple: the free surface elevation changes linearly from upstream to downstream. Figure 6 shows a smooth and consistent water level profile across the interfaces. As can be seen, the simulation results correctly reflect this simple flow structure as expected.
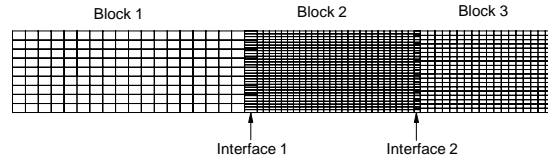

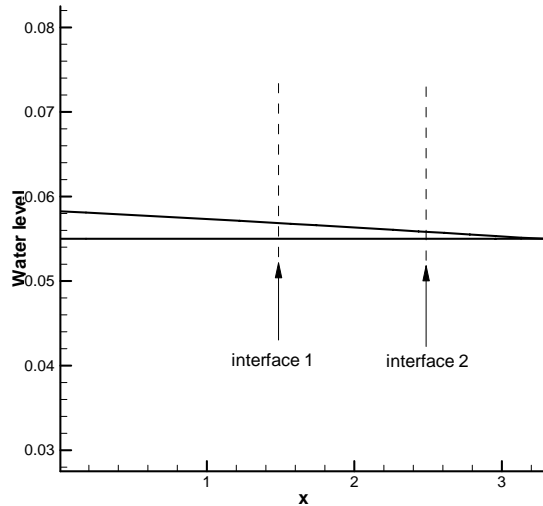Fig. 5 Mesh and layout of a straight channel

Fig. 6 Water level profiles in the longitudinal direction

B. Straight Channel with a Spur Dike

The second test case is a straight flume with a spur dike based on the experiment conducted by Rajaratnam and Nwachukwu [25]. The flume is 0.914m wide, 37m long and 0.76m deep. The experimental run A1 is simulated here. The flume bed and

walls are smooth and the Manning's coefficient is 0.011. The spur dike is an aluminum plate with a thickness of 3mm and a projection length b of 0.152m. The simulated reach is 6m long. A discharge of 0.0453 m^3/s is imposed at the upstream end of the channel, while a water surface elevation of 0.189 m is specified at the downstream of the channel.

The spur dike has significant influences on the flow patterns around it. It causes a recirculation zone downstream with a length of about 12b. Two regions of the disturbed flow, a deflected flow region and a shear layer, can be identified.

In order to investigate the efficiency improved by local mesh refinement, a single-block coarse mesh (43×9), a single-block fine mesh (77×20) and a two-block mesh (43×9+37×14) in which the CIM is used, are generated, as shown in Figure 7. In the two-block mesh, the resolution of block 1 (main channel) is the same as that of the single-block coarse mesh, while block 2 (dike zone) has the same mesh resolution as single-block fine mesh. Figure 8 compares the measured and simulated velocities at the cross sections: $x = 2b$, $4b$, $6b$, and $8b$ (b is the length of the dike). Without sufficient mesh resolution, the single block coarse mesh predicted the circulation zone with larger errors. The use of the two-block mesh improves results significantly. The best results are obtained using the single-block fine mesh, as expected. The results obtained with two-block mesh which uses considerably less mesh nodes are quite close to those obtained with the single-block fine mesh.
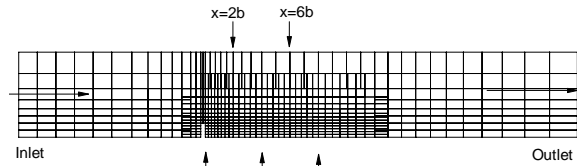
(d) Two-block Mesh

Fig. 7 Straight Channel with Spur Dike
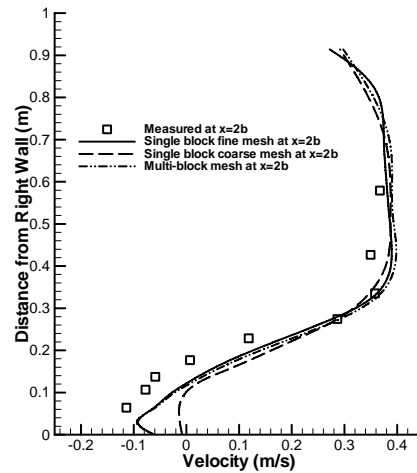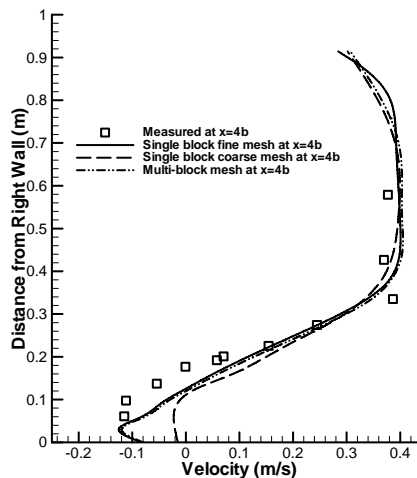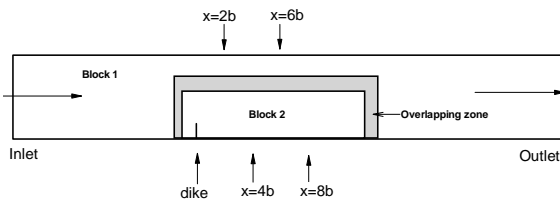
(a) Layout
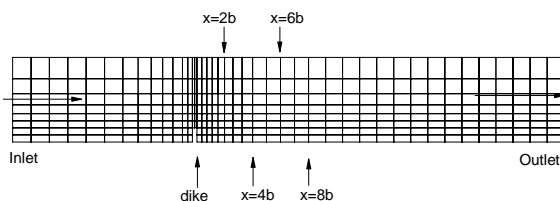
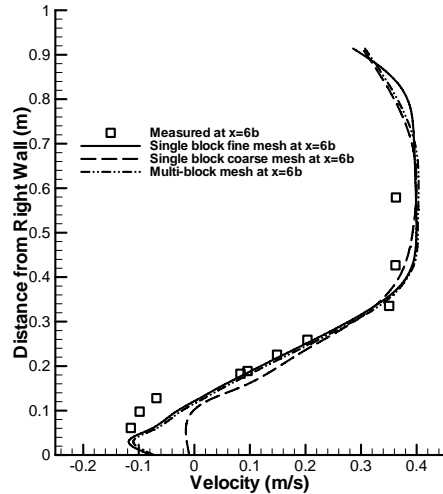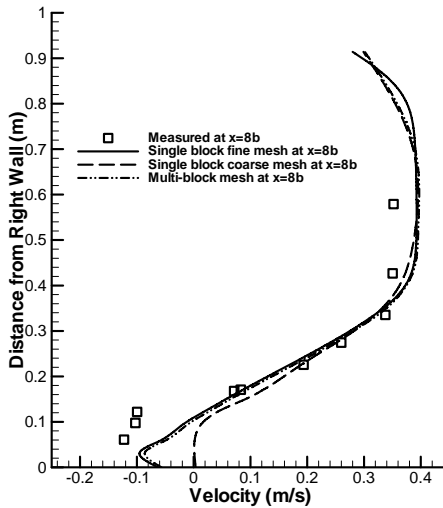
(b) Single-block Coarse Mesh
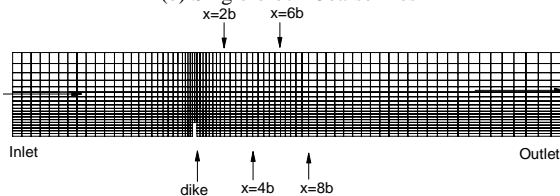
(c) Single-block Fine Mesh

(a) at x = 2b
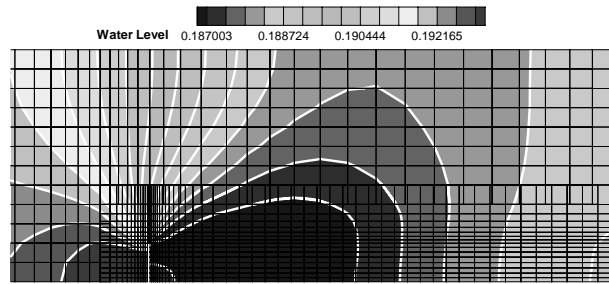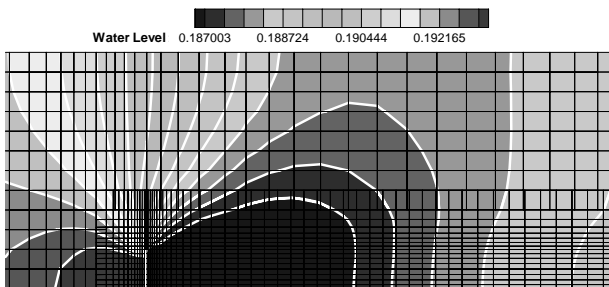

(b) at x = 4b

(c) at x = 6b

(d) at x = 8b

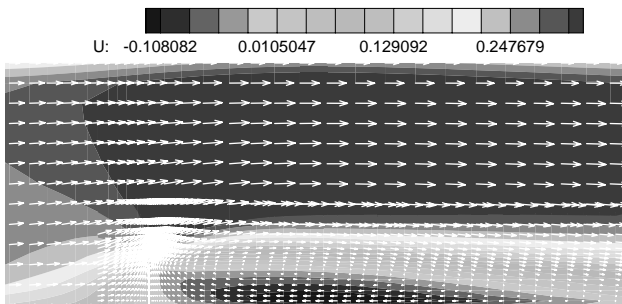Fig. 8 Velocity Profiles

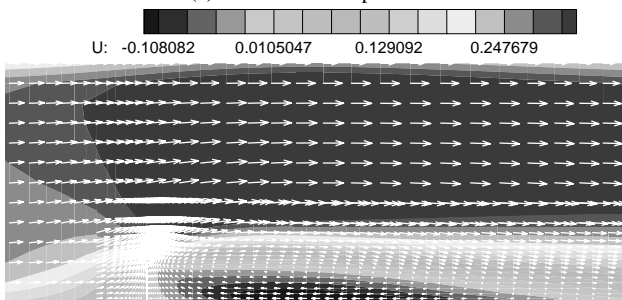(a) Consistent Interpolation

(b) Lagrangian interpolation

Fig. 10 Local water surface distribution

(a) Consistent Interpolation

(b) Lagrangian Interpolation

Fig. 11 Local velocity pattern

The comparison of the LIM and the CIM is also investigated based on another two-block mesh ($54 \times 13 + 58 \times 17$), as shown in Figure 9. Figure 10 and Figure 11 show the local water surface distribution and the velocity pattern within the circulation zone of the dike, respectively. As can be seen, the flow variables (free water surface elevation and flow velocity) are distributed smoothly and consistently across the interfaces. The comparisons of the measured and simulated velocities are plotted in Figure 12. Obviously the CIM yields more accurate results.

Fig. 9 A Two-block Fine Mesh

(a) at x = 2b

(b) at x = 4b
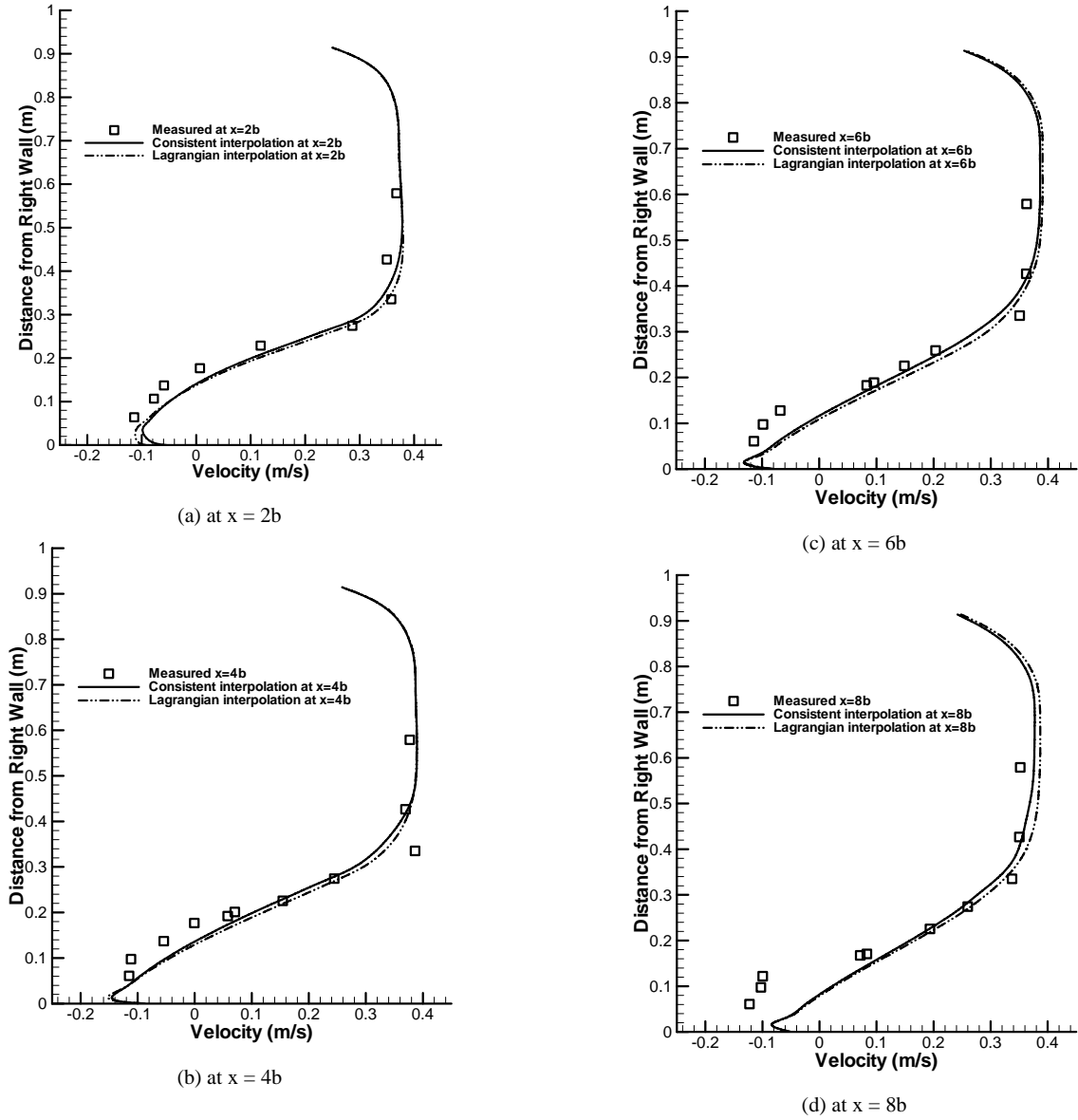

(c) at x = 6b

(d) at x = 8b

Fig. 12 Velocity Profiles

Figure 13 shows the mass conservation along the channel. For both methods, the mass error is less than 1%, which proved that the present multi-block algorithm is mass conservative. As can be seen, the CIM performed better in mass conservation due to the fact that it is conservative both in mass and momentum using the IC method.
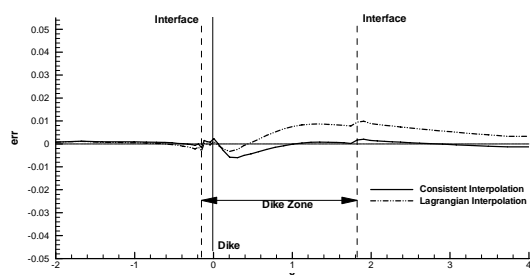
Fig. 13 Mass error along the channel

C. Bifurcation Channel with 90 Degree Angle

The numerical simulation of a divergent open channel flow is based on the experiment performed by Shettar and Murphy [26]. The main channel is 6m long with a 3m-long branch channel set at a right angle (90^0). The width and depth of both the main and the branch channel are 0.3m and 0.25m, respectively. The channel bed is finished with smooth cement plaster. The simulated reach of the main channel is 1.2m long and that of the branch channel is 0.9m long. The Manning's coefficient is 0.011, and a discharge of $0.005673 \text{m}^3/\text{s}$ is applied at the upstream end of the main channel. The water surface elevation of 0.055m and 0.045m are imposed at the downstream of the main channel and the branch channel, respectively. At the junction, the water detaches from the corner with a circulation zone developed along the wall. Accordingly, the free water surface drops at the junction and then recovers at downstream of the main channel.

As shown in Figure 14, the effects of the mesh resolution is investigated based on a single block mesh (59×91) and a two-block mesh ($59 \times 25 + 67 \times 25$) which decomposed the solution domain into the main channel and the branch channel. Their mesh resolutions are the same except a slight difference in the distribution of mesh lines in x direction in the branch channel. The local distribution of water surface elevation and the velocity pattern are displayed in Figure 15 and Figure 16, respectively. As can be seen, the enforcement of the mass conservation across the interfaces successfully removed the inconsistency created by the interpolation. Figure 17 and Figure 18 show the comparisons of the water level profiles in the main channel (at $y = 0.0$m and $y = 0.3$m) and the branch channel (at $x = 0.45$m and $x = 0.75$m). Almost no difference can be identified between these two cases. It is shown that the proposed multi-block algorithm is quite stable. With the same mesh resolution, the two-block mesh is able to reproduce the results of the single block mesh.
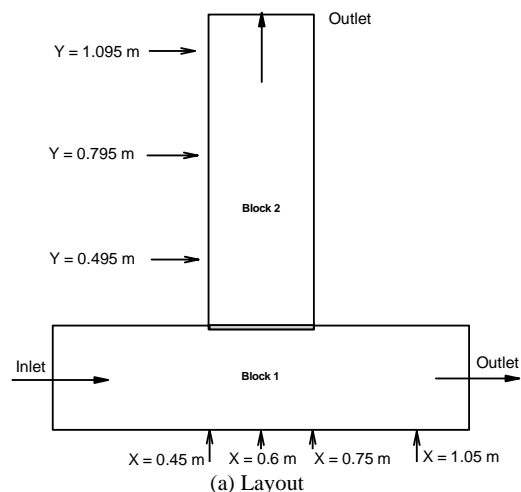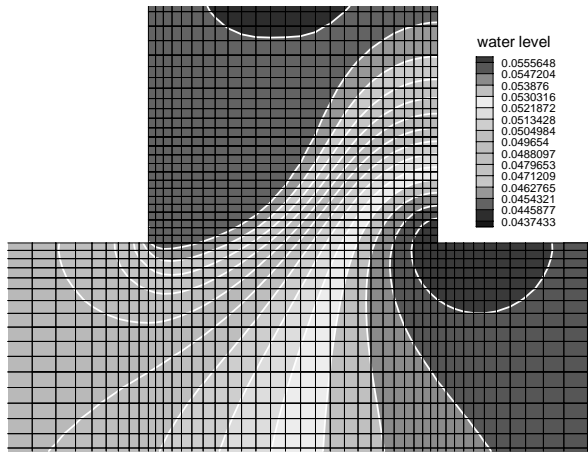

(a) Layout
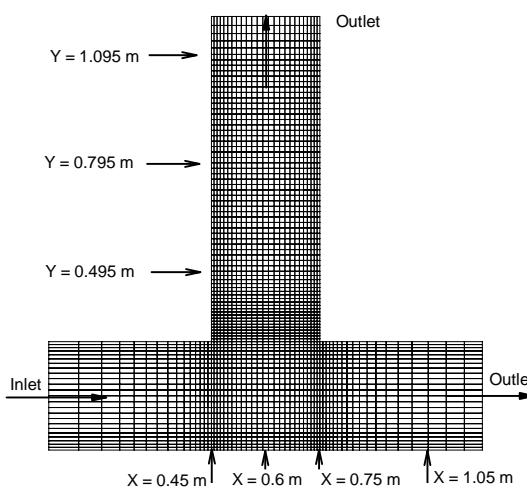
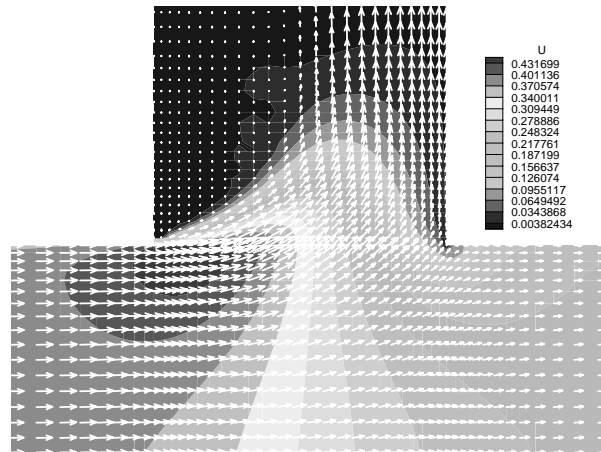(b) Single-block Mesh
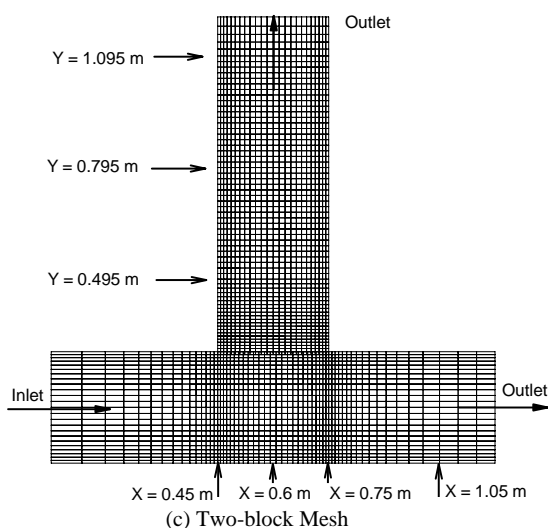
(c) Two-block Mesh

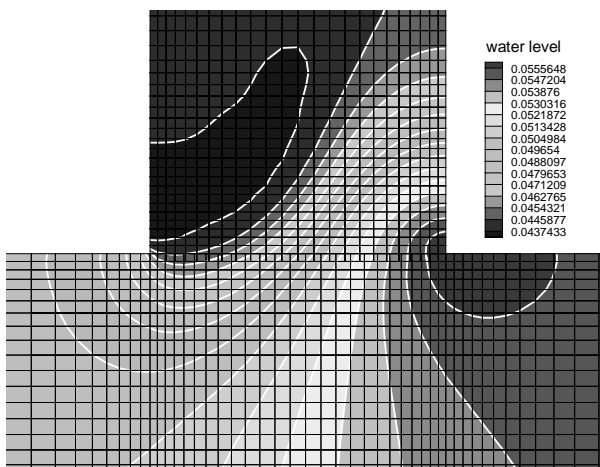Fig. 14 Single-block Mesh and Tow-block Mesh

(a) Single-block Mesh

(b) Two-block Mesh

Fig. 16 Local velocity pattern

(b) Two-block Mesh
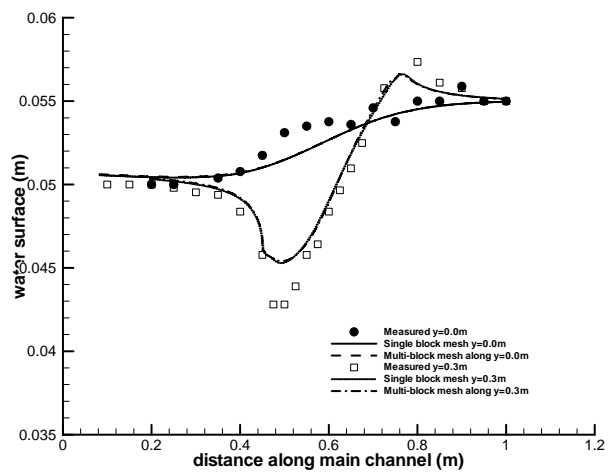
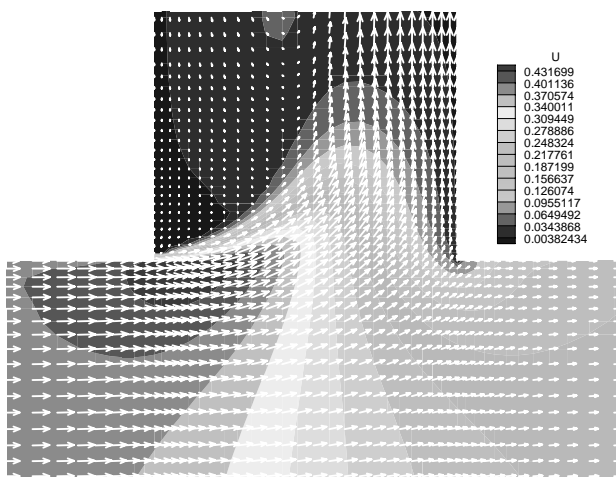Fig. 15 Local water surface distribution

Fig. 17 Water surface profile in the main channel
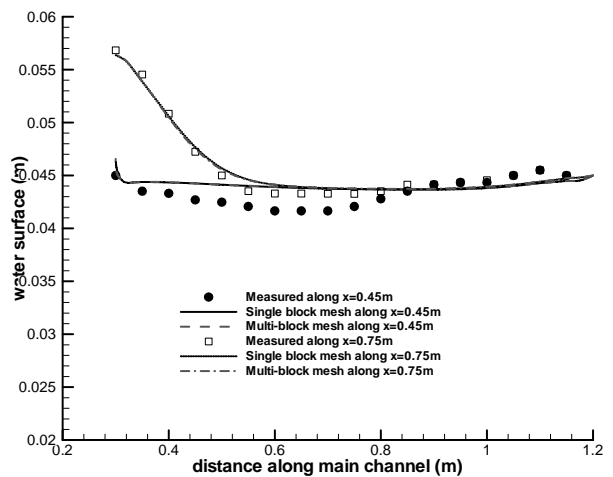

(a) Single-block Mesh

Fig. 18 Water surface profile in the branch channel

A four-block mesh ($80 \times 30 + 15 \times 25 + 15 \times 25 + 20 \times 25$) is used to compare the CIM and the LIM, as shown in Figure 19. Figure 20 and Figure 21 show the measured and simulated velocity profiles in the main channel (at $x = 0.45$m, 0.60m, 0.75m and 1.05m) and the branch channel (at $y = 0.495$m, 0.795m and 1.095m), respectively. In the main channel, there is no significant difference between the CIM and the LIM; while in the branch channel, the CIM performed better.
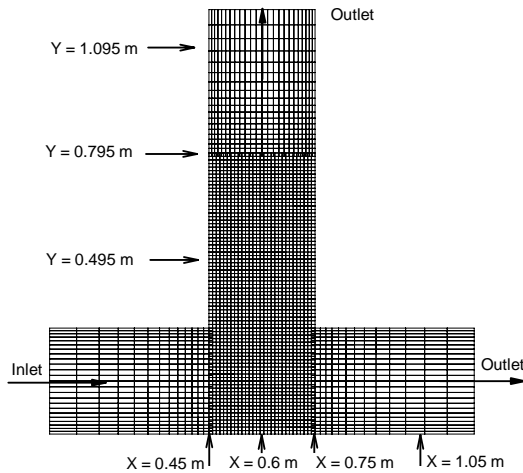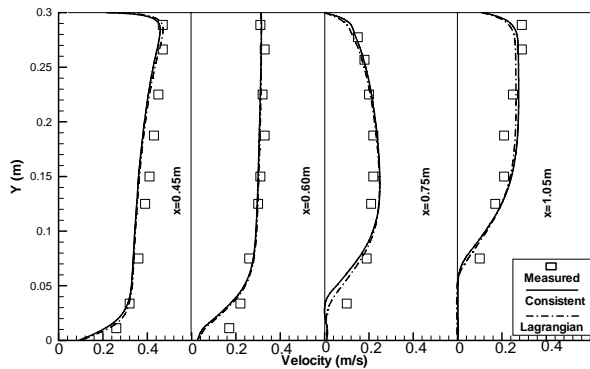

Fig. 19 Four-block Mesh

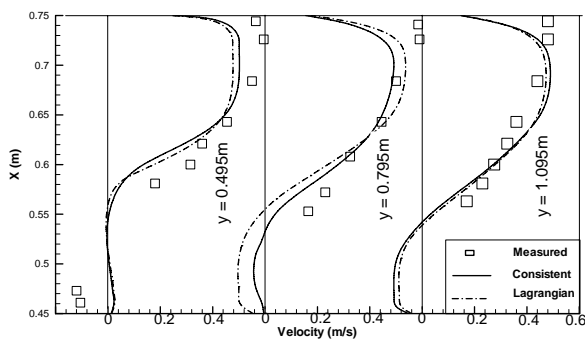Fig. 20 Velocity profiles in the main channel

Fig. 21 Velocity profiles in the branch channel

D. Sudden-Expansion Channel

The flow simulation in a sudden-expansion flume is based on the experiment measured by Xie [35]. The flume is made of concrete bed and walls, with a bed slope of 1/1000, a length of 18m and a width of 1.2m. The sudden expansion width ΔH is 0.6m wide. One experiment with the flow discharge of 0.01815m^3/s, the approach velocity of 0.3m/s and the approach Froude number of 0.3 is simulated. As shown in Figures 22 and 23, the flume is decomposed into two blocks with mesh sizes of 15×91 and 20×60, respectively. Obviously, this case is more challenging because the interface lies in the shear layer rather than the expansion section.
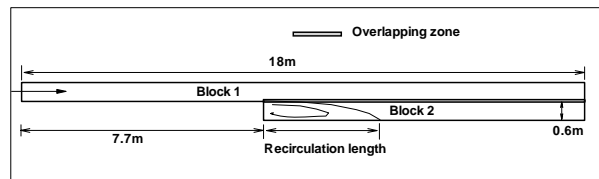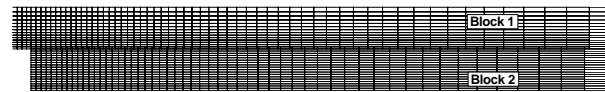

Fig. 22 Layout of sudden-expansion channel

Fig. 23 A Two-block Mesh

Figure 24 compares the velocity patterns from the CIM and the LIM. No significant difference is found between them. Figure 25 shows the comparisons of the simulated and measured velocities at $x = 0.0$m, 1.0m, 2.0m, 3.0m, 4.0m and 5.0m. As can be seen, the overall agreement between the simulated results and the measured data are quite good. Due to the application of the zero-equation eddy viscosity model, the recirculation length is over-predicted compared to the measured data which indicated a length of 4.6m equivalent to 7.83 ΔH. Jia et al. [17] applied the single-block version of CCH2D model to this case and obtained more accurate results with the use of $k - \varepsilon$ turbulence model. It is shown that compared to the IIM, the CIM predicted the velocity profiles in the shear layer more accurately.
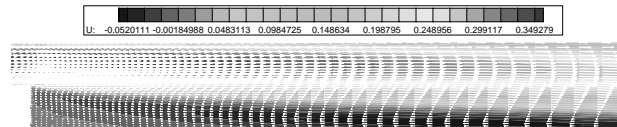
(a) Consistent Interpolation
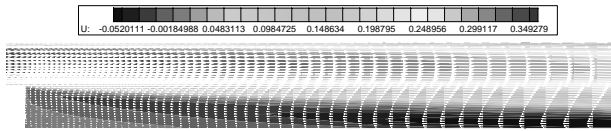
(b) Lagrangian Interpolation
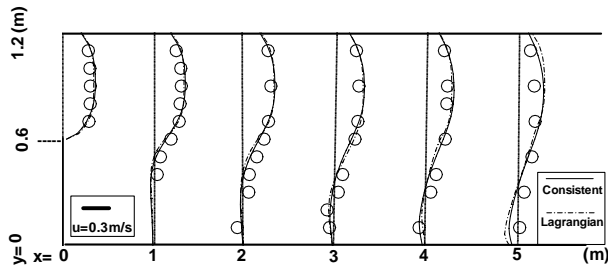Fig. 24 Local velocity pattern

Fig. 25 Velocity profiles

V. Conclusions

A conservative multi-block algorithm has been developed for two-dimensional hydrodynamic model. Both the LIM and the CIM are used to transfer information between neighboring blocks. Different from the LIM, which directly interpolates solutions at the interpolation nodes with assumed distribution, the CIM solves the momentum equations within the auxiliary elements constructed for the interpolation nodes. With the IC method, both methods are mass-conservative across the interfaces, but the CIM is capable of maintaining the momentum conservation as well. Although it needs more computational efforts, the CIM produces physically more reasonable results. Several flow simulation examples are used to test the multi-block algorithm presented in this paper. It is shown that the CIM yields more accurate results than the LIM. The current multi-block algorithm is capable of efficiently producing results whose accuracy is comparable to those obtained with the single-block meshes.

Acknowledgment

References

[1]. Benek, J.A., Steger, J.L., and Dougherby, F.C. (1983), "A Flexiable Grid Embedding Technique with Application to the Euler Equations", *AIAA* Paper 83-1944, 1983.

[2]. Berger, M. (1987), "On Conservation at Grid interface", *SIAM J. Numer. Anal*, 24(5).

[3]. Brakkee, E., Wesseling, P., and Kassels, C.G. (2000), "Schwarz domain decomposition for the incompressible Navier-Stokes equations in general coordinates", *Int. J. Numer. Methods Fluids*, 32:141-173.

[4]. Caruso, S.C.(1985), "Adaptive grid techniques for elliptic fluid-flow problems", Ph.D. Dissertation, Department of Mechanical Engineering, Stanford University, Stanford, CA.

[5]. Chen, H.C., and Chen, M.(1998), "Chimera RANS simulation of a berthing DDG-51 ship in translational and rotational motions", *Int. J. Offshore and Polar Engrg*., 8(3): 182-191.

[6]. Chen, H.C., and Liu, T.(1999), "Turbulent flow Induced by Full-scale Ship in Harbor", *ASCE, J. Engrg. Mech.*,125(7): 827-835.

[7]. Chesshire, G., and Henshaw, W.D.(1994), **"**A scheme for conservative interpolation on overlapping grids", *SIAM J. of Scientific Computing*, 15(4): 819-845.

[8]. Francisco, J.S., and Sabadell, F.J.(2000), "The multi-block method---a new strategy based on domain decomposition for the solution of wave propagation problems", *Int. J. Numer. Methods Engrg*., 49: 1353-1376.

[9]. Furukawa, M., Yamasaki, M., and Inoue, M.(1989), "A zonal approach for solving the Navier-Stokes Equations using a TVD Finite Volume Method", International Symposium on CFD, Nagoya, Nagoya Trade & Industry Center, Japan, August 28-31, 1989.

[10]. Gresho, P.M. and Sani, R.L.(1987), "On pressure boundary conditions for the incompressible Navier-Stokes equations", *Int. J. Numer. Methods Fluids*, 7: 1111-1145.

[11]. Henshaw, W.D. (1985), "Part I: The numerical solution of hyperbolic systems of conservation laws. Part II: Composite overlapping grid techniques", Ph.D. Dissertation, California Institute of Technology, Pasadena, CA, 1985.

[12]. Henshaw, W.D. (1994), "A fourth-order accurate method for the incompressible Navier-Stokes equations on overlapping grids", *J. Comp. Phys*, 113(1):13-25.

[13]. Hessinius, K., and Rai, M. (1986), "Three Dimensional Conservative, Euler Computations using Patched Grid Systems and Explicit Methods", AIAA Paper 86-1088, 1986.

[14]. Jia, Y.F., and Wang, S. S-Y.(1999), "Numerical Model for channel flow and morphological changes studies", *ASCE J. Hydraulic Engrg*, 125(9): 924-933.

[15]. Jia, Y.F., and Wang, Sam S.Y. (2001a), "CCHE2D: Two-dimensional Hydrodynamic and Sedimenst Transport Model for Unsteady Open Channel Flows Over Loose Bed", Technical Report, NCCHE-TR-2001-1, Aug. 2001.

[16]. Jia, Y.F., and Wang, Sam S.Y. (2001b), "CCHE2D Verification and Validation Tests Documentation", Technical Report, NCCHE-TR-2001-2, Aug. 2001.

[17]. Jia, Y.F., Wang, S.S.Y., and Xu, Y.C (2002), "Validation and Application of a 2D Model to Channels with Complex Geometry", *Int. J. Comp. Engr. Sci*., 3(1): 57-71.

[18]. Klopfer, G.H., and Molvik, G.A. (1991), "Conservative multi-zonal interface algorithm for 3D Navier-Stokes equations", AIAA paper 91-1601-CP, AIAA 10th CFD Conference, Honolulu, Hawaii.

[19]. Meakin, R.L. (1986), "Application of boundary conforming coordinate and domain decomposition principles to environmental flows", Ph.D. Thesis, Department of Civil Engineering, Stanford University.

[20]. Meakin, R.L., and Street, R.L. (1988), "Simulation of environmental flow problems in geometrically complex domains, part 2: A domain-splitting method", *Compu. Methods Appl. Mech. Eng.*, 68: 311-331.

[21]. Moon, Y. J. and Liou, M.-S. (1989), "Conservative treatment of boundary interfaces for overlaid grids and multi-level grid adaptations", AIAA Paper 89-1980-CP, AIAA 9th CFD Conference, Buffalo, NY.

[22]. Perng, C.Y., and Street, R.L. (1991), "A coupled multi-domain-splitting technique for simulating incompressible flows in geometrically complex domains", *Int. J. Numer. Methods Fluids*, 13: 269-286.

[23]. Rai, M. M. (1986a), "A conservative treatment of zonal boundaries for Euler equation calculations", *J. Comput. Phys.*, 62: 472-503.

[24]. Rai, M.M. (1986b), An Implicit Conservative Zonal Boundary Scheme for Euler Equation Calculations, *Comp. Fluids*, 14: 295-319.

[25]. Rajaratnam, N., and Nwachukwu, B.A.(1983), "Flow near groid-like structures", *J. of Hydraulic Engineering*, 109(3): 463-481

[26]. Shetter, A.S., and Murphy, K.K. (1996), "A numerical study of division flow in open channels", *Journal of Hydraulic Research*, IAHR, 34(5): 651-675.

[27]. Sheng, C., Taylor, L.K., and Whitefield, D.L. (1995), "Multiblock multigrid solution of three-dimensional incompressible turbulent flows about appended submarine configurations", AIAA-95-0203, 33rd Aerospace sciences meeting and exhibit, January 9-12, 1995, Reno, NV.

[28]. Sinha, K. S., Sotiropoulos, F., and Odgaard, A. J.(1998), "Three-dimensional numerical model for flow through natural rivers", *J. Hydr. Engrg.*, ASCE, 124(1):13-24.

[29]. Steger, J.L. (1991), "Thoughts on the Chimera Method of Simulation of Three-Dimensional Viscous Flow", in Proceedings, CFD symposium on Aeropropulsion, Cleveland, Ohio, NASA CP-3078, 1991, 1-10.

[30]. Tu, J.Y., and Fuchs, L.(1992), "Overlapping grids and multi-grid methods for 3D unsteady flow calculation in I.C engine", *Int. J. Numer. Methods Fluids*, 15: 693-714.

[31]. Van Leer, B. (1982), "Flux-Vector Splitting for the Euler Equations", Lecture Notes in Physics, Vol. 170: 507-512.

[32]. Wang, S.S.Y., and Hu, K.K. (1997), "Improved methodology for formulating finite-element hydrodynamic models", *Finite element in fluids*, T.J.Chung, ed., Vol. 8, Hemisphere Publishing Corp., 457-478.

[33]. Wang, Z.J. (1994), "Conservative Chimera for 3D Euler Equations on Structured/Structured, Structured/Unstructured Grids", Proceedings of the 2nd Overset Composite Grid and Solution Technology Symposium, Ft Walton Beach, Florida, October 1994.

[34]. Wright, J., and Shyy, W.(1993), "A pressure-based composite grid method for the Navier-Stokes equations", *J. Comp. Phy.*, 107: 225-238.

[35]. Xie, B.L.(1996), "Experiment on flow in a sudden-expanded channel", *Technical Report*, Wuhan University of Hydraulic and Electric Engineering, China.

[36]. Zang, Y., and Street, R.L. (1995), "A composite multi-grid method for calculating unsteady incompressible flows in geometrically complex domains", *Int. J. Numer. Methods Fluids*, 20: 341-361.